Journal of Applied Polymer Science

Effect of electrospun fibers of polyhydroxybutyrate filled with different organoclays on morphology, biodegradation, and thermal stability of poly(ε-caprolattone)

Carla Marega, Antonio Marigo
Dipartimento di Scienze Chimiche, Università di Padova, via Marzolo 1 I-35131, Padova, Italy
Correspondence to: C. Marega (E-mail: carla.marega@unipd.it)

ABSTRACT: The properties of nanocomposites of poly(ε-caprolattone) (PCL) were studied, the pristine PCL was implemented with the introduction of electrospun fibers of polyhydroxybutyrate (PHB), containing a cationic (Cloisite) or an anionic (Perkalite) clay. These multicomponent composites containing a very low amount of clay confined in fibers are different from usual nanocomposite materials containing clay dispersed in the polymer matrix, which are produced by solvent casting or melt extrusion. To analyze the influence of the different fillers on the final composite, a preliminary study on PHB cast films and fibers prepared from the same solution was carried out, and then a thorough analysis was accomplished of the behavior of these particular nanocomposites PCL/PHB fibers/clay to elucidate the effects of the filled electrospun fibers on the PCL matrix. The structure and morphology of the samples were characterized by wide-angle X-ray diffraction and small angle X-ray scattering; differential scanning calorimetry and thermogravimetric analysis were used to understand the influence of the fillers on the thermal behavior and stability; mechanical properties were evaluated and biodegradation studies were carried out. The PHB electrospun fibers and the fractured surface of the final composites were examined by scanning electron microscopy. © 2015 Wiley Periodicals, Inc. J. Appl. Polym. Sci. **2015**, *132*, 42342.

KEYWORDS: biodegradable; composites; X-ray

Received 23 June 2014; accepted 10 April 2015
DOI: 10.1002/app.42342

INTRODUCTION

Although designed and tested for decades, biodegradable polymers are gaining importance as possible substitutes for synthetic plastics, especially for environmental reasons, due to the possibility that artifacts made from them are subjected to biodegradation—natural or bacterial—which gives rise to products harmless or even beneficial to the environment. It is a considerable advantage since the main problem of traditional plastic materials derives from the fact that the final products are indestructible by natural and hardly disposable.

In fact, biopolymers are a class of materials that are extremely interesting because it is possible to get them from renewable resources; furthermore, their physicochemical properties can be modified respond to multiple application needs.

Among the biocompatible and biodegradable polymeric materials, the class that has attracted most interest is that of aliphatic polyesters, whose applications include conventional sectors such as agriculture, packaging, fibers, and biomedical areas.

The polyhydroxyalkanoates (PHAs) are a group of biodegradable and biocompatible polyesters[1,2] synthesized by a large number of intracellular bacteria (e.g., *Alcaligenes eutrophus* or *Bacillus megaterium*) for which they constitute an important energy supply. The monomer composition of PHAs is determined by the relative concentration of carbon sources available or by the conditions in which fermentation takes place. More than a hundred different types of monomers are known, each of which has a specific structure.[1]

The most important of the PHAs is polyhydroxybutyrate (PHB),[3–10] a semicrystalline thermoplastic polyester identified in 1926 by the Institute Lemoigne Pasteaur as a constituent of the microorganism Bacillus megaterium.[3] PHB possesses a remarkable crystallization rate, high degree of crystallinity (55–80%), high melting temperature ($T_m \sim 180°C$), and a glass transition under room temperature ($Tg \sim 4°C$); however, its brittle behavior and lack of melt stability have seriously restricted its use.[4]

Another polymer of great interest, even though it is a synthetic one, is poly(ε-caprolattone) (PCL); it is a linear semicrystalline

Additional Supporting Information may be found in the online version of this article.

Table I. Samples Composition

Sample	Type of samples	Organoclay
PHBp	Powder	/
PCLp	Pellet	/
PHBcf	Cast film	/
PHBcf2CL	Cast film	2% cloisite
PHBcf5CL	Cast film	5% cloisite
PHBcf2PK	Cast film	2% perkalite
PHBcf5PK	Cast film	5% perkalite
PHBfb	Fiber	/
PHBfb2CL	Fiber	2% cloisite
PHBfb5CL	Fiber	5% cloisite
PHBfb2PK	Fiber	2% perkalite
PHBfb5PK	Fiber	5% perkalite

polyester, characterized by a low glass transition temperature (T_g −60°C) and produced by ring-opening polymerization of ε-caprolactone.

It is biocompatible and biodegradable, either through hydrolytic or enzymatic cleavage along the macromolecular chain. Its potential uses are currently being examined in biodegradable packaging materials,[11] in pharmaceutical controlled release systems, and other medical applications.

It can therefore be understood that as is now widely used for synthetic plastics, one thinks of the enhancement of the properties of PHB[4,12–15] and PCL[16–29] by preparation of nanocomposites, trying to modulate the characteristic of biodegradability of the material and enhance its mechanical properties, thermal stability, gas barrier properties, electrical properties, and also the biodegradation rate.

In some recent articles, it is already reported the preparation of nanocomposites of PCL via the introduction, into the polymeric matrix, of nylon fibers obtained by electrospinning,[30,31] with the intent of improving the mechanical properties and tuning the biodegradation rate of the nanocomposite; in this article, we want to extend the study to multicomponent composites of PCL filled with fibers of PHB, in which a cationic (Cloisite) or an anionic (Perkalite) clay is introduced.

The purpose of this article is to verify if the new multicomponent composites can have biodegradation behavior and thermal and mechanical properties different than those of the traditional composites prepared by solvent casting.

In particular, it is interesting to investigate if a filler consisting of PHB, a biodegradable polymer with better thermal properties than the matrix of PCL, can improve the thermal properties and the biodegradation rate of the composite.

The further addition of a very low percentage of clay (which represents the nondegradable part of the final composite) has the purpose of enhancing mechanical properties.

To have a clear understanding of the influence of the different fillers on the final composite, a preliminary study on PHB cast films and fibers (prepared from the same solution) was carried out, then a thorough analysis of the behavior of the nanocomposite PCL/PHB fibers/clay was accomplished.

The structure and morphology of the samples were characterized by wide-angle X-ray diffraction (WAXD) and small angle X-ray scattering (SAXS). Biodegradation studies were then carried out with respect to time and the influence of the structure on the degradation of nanocomposites was studied by WAXD. Differential scanning calorimetry (DSC) and thermogravimetric analysis (TGA) was used to understand the influence of fillers on thermal behavior and stability.

The PHB electrospun fibers and the fractured surface of the final composites were examined by scanning electron microscopy (SEM).

EXPERIMENTAL

PHB in the form of powder was purchased from Sigma Aldrich (Milano/Italy) and used as received. This natural-origin polymer is reported by the producer to have $T_m = 172$°C.

Weight average molecular weight ($\overline{M}w$) and number average molecular weight ($\overline{M}n$) were determined by gel permeation chromatography (GPC) to be, respectively, 242,920 g/mol and 227,900 g/mol. GPC measurements were obtained with a GPC chromatograph Agilent 1260 Infinity equipped with a Phenomenex Phenogel 5 MXM and with a refractive index detector, chloroform was used as solvent at 30°C.[32]

PCL in the form of pellets was purchased from Sigma Aldrich (Milano/Italy) and used as received; according to the supplier, the weight average molecular weight ($\overline{M}w$) and number average molecular weight ($\overline{M}n$) were, respectively, 48,000–90,000 and 40,000–50,000 g/mol.

The multicomponent composites were prepared using PCL as matrix and the fibers of PHB containing two organoclays as filler.

The first clay was the most widely used cationic one, Cloisite 20A (Southern Clay Products), and the other was the organically modified layered double hydroxide Perkalite (Akzo Nobel), an anionic clay. Cloisite 20A is a commercial montmorillonite organomodified by ion-exchange with dimethyl dehydrogenated tallow quaternary ammonium salt. Perkalite is a synthetic hydrotalcite clay, treated with a proprietary composition of anionic surfactants.[33]

A 8 wt % PHB solution in chloroform/dimethylformamide (90/10, wt/wt) was prepared; the percentage of PHB was chosen, after testing solutions at 6 and 10%, as the most suitable to obtain electrospun fibers.

The solution was then divided into five parts, the first was used as obtained and the others were added, respectively, with 2 and 5% Cloisite and with 2 and 5% Perkalite. From these solutions, cast films and fibers were prepared whose characteristics are shown in Table I.

The films of nanocomposite and of neat PHB were prepared by a solvent casting method and the entire procedure was carried out in a crystallizer to obtain a greater surface area.

Table II. Sandwiched Composites

Sample	Type of fiber	Fiber content	Organoclay content
PCL	/	/	/
PCL/PHB	PHBfb	3.5%	/
PCL/PHB_2CL	PHBfb2CL	3.5%	2% cloisite
PCL/PHB_5CL	PHBfb5CL	3.5%	5% cloisite
PCL/PHB_2PK	PHBfb2PK	3.5%	2% perkalite
PCL/PHB_5PK	PHBfb5PK	3.5%	5% perkalite

The solution was stirred and heated at about 50°C for 2 h and the film was obtained by removal of the solvent.

PCL pellets were compression molded into films by the application of heat and pressure in a press (Alfredo Carrea, Genova, Italy), the polymer was melted at 90°C and then left inside the press until cooling to room temperature. Films of 0.5 mm thickness were obtained.

Preparation of sandwiched samples was made by impregnation of the electrospun fibers mat with the molten PCL, by compression molding.[30,31,34] The PHB nanofiber mat was sandwiched between PCL films at 90°C, PCL was melted and percolated between the voids in the mat, constituting a continuous phase in which the fibers were dispersed.

A neat PCL sample and five composites, differing by formulation (Table II), were prepared in order to evaluate the effect of PHB fibers, containing different percentage of the two types of clay, on the morphology and performance of the composite materials.

To determine the actual percentage of clay in the samples, thermogravimetric analysis was carried out, the results of which have confirmed that the percentages of residual material found in the different samples are consistent with those used for the preparation thereof.

Electrospinning

Electrospinning was carried out by processing the solution of neat PHB and the others added with clay with an applied voltage of 16 kV and tip to collector distance of 20 cm. Just after electrospinning, polymer nanofibers were placed under vacuum to remove residual solvent.

The morphology of electrospun polymer fibers was observed by polarized optical mircoscopy POM and SEM.

Wide-Angle X-ray Diffraction

WAXD patterns were recorded in the diffraction angular range 1.5–40° 2θ by a Philips X'Pert PRO diffractometer, working in the reflection geometry and equipped with a graphite monochromator on the diffracted beam (CuK_α radiation).

Transmission patterns were recorded in the diffraction range of 5–40° 2θ by a diffractometer GD 2000 (Ital Structures) working in a Seeman–Bohlin geometry and with a quartz crystal monochromator on the primary beam ($CuK_{\alpha 1}$ radiation).

The application of the least-squares fit procedure elaborated by Hindeleh and Johnson[35] gave the degree of crystallinity by weight which is then transformed in to the degree of crystallinity by volume (Φ_{WAXD}) when a comparison is needed.

Small Angle X-ray Scattering

The SAXS measurements were performed in an MBraun system by utilizing CuKα radiation from a Philips PW1830 X-ray generator. The patterns were recorded by a position sensitive detector in the scattering angular range 0.1–5.0° 2θ and corrected for the blank scattering. A constant continuous background scattering[36] was subtracted and the obtained intensity values $\tilde{I}(s)$ were smoothed, in the tail region, with the aid of the $s\tilde{I}(s)$ versus $1/s^2$ plot.[37] Then Vonk's desmearing procedure[38] was applied and the one-dimensional scattering function was obtained using the Lorentz correction: $I_1(s) = 4\pi s^2 I\ (s)$, where $I_1(s)$ is the one-dimensional scattering function and $I(s)$ is the desmeared intensity function.

The sum of the average thicknesses of the crystalline and amorphous layers was determined as the Bragg identity period (or long period) D of the function $I_1(s)$.

SAXS Data Analysis

The evaluation of the SAXS patterns according to some theoretical distribution models[39] was carried out referring to the Hosemann model,[40] which assumes the presence of lamellar stacks having an infinite side dimension. This assumption takes into account a monodimensional electron density change along the normal direction to the lamellae.

The fitting procedure[39] of the calculated one-dimensional scattering function with the experimental one allows to optimize the values of the thicknesses and distributions of the crystalline and amorphous layers, the long period and the crystallinity, along with their distribution, associated to lamellar stacks.

Polarized Optical Microscopy

POM analysis was performed by a Leica DM4000 M microscope equipped with a Leica DFC camera.

Scanning Electron Microscopy

Scanning electron microscopy (SEM) pictures were obtained by an XL30 scanning electron microscope (Philips). All considered specimens were gold coated.

Thermal Analysis

DSC measurements were carried out by a model 2920 calorimeter (TA Instruments) operating under N_2 atmosphere. The samples, weighing about 5 mg, were closed in aluminum pans.

A heating rate of 10°C/min up to 200°C was set in order to observe the polymer melting peak for the fibers of PHB and the sandwiched samples.

Indium of high purity was used for calibrating the DSC temperature and enthalpy scales. Thermogravimetric analysis (TGA) was performed with a TA Instrument SDT 2960 simultaneous TG/DSC system. The scans were recorded at a heating rate of 10°C/min in a temperature range from 30 to 600°C. Experiments were done under air.

The onset of the degradation was calculated as the intersection between the starting mass line and the line of maximum gradient tangent to the TG curve, the temperature corresponding to

the maximum of the derivative of the TG curve with respect to temperature was indicated as the degradation temperature (T_{deg}).

Mechanical Properties

The tensile properties of the sandwiched samples (dimensions 30 × 10 × 1 mm) were measured using an Instron Model 3345 mechanical tester at room temperature.

The cross-head speed was 5 mm/min and five samples were tested for each composition. The stress and the strain at yield and break and Young's modulus were measured with relative errors of max 4%.

Biodegradation Studies

Biodegradation studies were carried out in an all-purpose gardening soil (pH = 7.0, used as purchased from a gardening shop) kept moist at 100% relative humidity. The structure of the composite samples was evaluated before, during, and after degradation. The samples were taken out every 20 days until the end of the experiments and the percentage of weight loss was regarded as the measure of biodegradation.

A particular care was taken not to disperse small fragments that could arise during the handling of the samples which preceded the mass measurements.

RESULTS AND DISCUSSION

In this work, we have characterized PHB in the form of cast films and fibers and finally the sandwiched composites, consisting of PCL matrix and PHB fibers filled with Cloisite or Perkalite. The preparation of the composites is an original way to add nanoparticles in a polymer matrix, without preparing the samples from solution or by extrusion; in this case, the nanofillers remain confined within the fibers because the melting temperature of PHB is higher than that of PCL.

Since the amount of PHB fibers is 3.5% in PCL and that of clay 2 or 5% in the fibers, it is easy to establish that the total percentage of nanofillers in the final composite is very low.

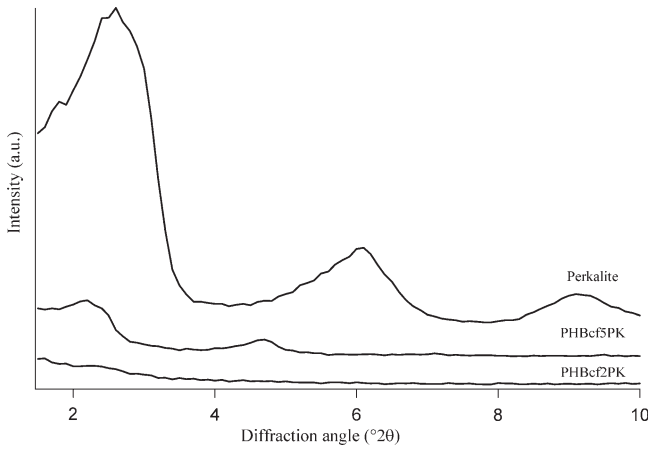

Figure 1. WAXD traces of cast film composites and of neat Perkalite in the angular region of the basal peaks of clay.

Table III. Calculated Interlayer Space of Neat Clays and Film Nanocomposites

Sample	2θ	Interlayer space (Å)
cloisite	3.5	25.2
perkalite	2.6	34
PHBcf5CL	2.4	36.8
PHBcf5PK	2.2	40.1

PHB Films by Solvent Casting and Electrospun Nanofibers

The preparation of the samples in the form of cast film was used in particular for the study of the phenomenon of biodegradation of PHB, with and without clay, prepared by solution, because the morphology of the samples, produced in the form of fiber, makes especially difficult the collection of fragments in which the sample is divided after the stay in soil and then it prevents a correct analysis of the weight loss during the biodegradation process.

The characterization of films and fibers allows also to highlight the difference between the two macroscopic morphologies from the point of view of the influence of clay on the structure of PHB.

For the calculation of the degree of crystallinity of cast film samples, WAXD patterns were recorded in the diffraction angular range 10–40° 2θ. The diffraction patterns of the samples exhibit the typical pattern of PHB and significant changes to the profile of the matrix were not detected. The results obtained are reported in Supporting Information, Table 1S.

The results show the same trend for both clays: while the nanocomposites with 2% clay show an increase, those loaded with 5% show a decrease of crystallinity. The phenomenon can be justified by the fact that the fillers normally exert a double effect on the crystallization of the polymer matrices. On one hand, they act as nucleating agents, favoring the formation of nuclei of crystallization and so increasing the rate of crystallization. On the other hand, however, the presence of the inorganic particles interferes with the movement of the macromolecular chains, acting as a hindrance to their regular alignment.[41]

WAXD analysis allows to identify the clay basal peaks in the small angle region where they appear (2.5–3.5° 2θ), corresponding to angular values of the interlayer space characteristic of the clay crystallographic planes 001 (Supporting Information, Figure 1S).

A comparison between the diffraction spectra of neat clays and cast films allows to establish a shift of the basal peak 001 toward smaller angles (Figure 1), although it is possible to determine the interlayer space only for nanocomposites loaded with 5%; in fact, the basal peak in those loaded with 2% is too weak.

The obtained results are reported in Table III.

The increase in the interlayer space detected in the samples containing the 5% filler, compared to that of the neat clay, indicates that during the preparation of the solution, a phenomenon of intercalation occurs, due to the good affinity between the polymer and the clay, and the splitting of the layers of clay persists during the cast film formation.

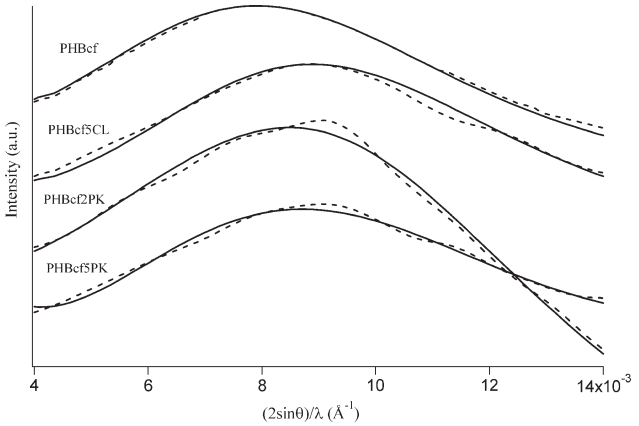

Figure 2. SAXS patterns (dotted lines) of cast film composites. Traces calculated during the fitting procedure (solid lines) are also shown.

SAXS was used to investigate the semicrystalline framework of the material on the scale of lamellar stacks. SAXS experimental patterns can be seen in Figure 2 and were fitted according to the method,[39] which was proved[42–44] to reliably determine the morphological parameters, relating to the lamellar stacks, that are shown in Table IV.

It was not possible to apply the fitting procedure to the sample PHB2CL because its SAXS pattern was too poor.

From the comparison of the data reported in Supporting Information, Table 1S and Table IV, it is possible to point out that Φ_{SAXS} is always a little bit larger than Φ_{WAXD}.

Actually the different values of crystallinity obtained with the two techniques are due to the fact that by WAXD analysis, it is possible to detect all the regions contributing to the semicrystalline framework, including the amorphous phase located outside the lamellar stacks, while SAXS analysis allows to consider only the crystallinity related to the morphology of the lamellar stacks.[45]

It is possible to observe that the number of lamellae per stack is low as well as the lamellar thickness; therefore, it can be concluded that the preparation of cast films hinders the formation of extended lamellar stacks and leads to the formation of thin lamellae.

All the loaded cast films retain the same long period; besides PHB2PK shows a broadening of the SAXS signal. This indicates that, for this sample, the lamellar stacks are less homogeneous in size and morphology; it is so possible to assume that the formation of thin lamellae is even more evident for PHB2CL, resulting in an SAXS peak of low intensity and large broadening such as to make impossible an accurate determination of both size and distribution of the lamellae and indicating a disruption of the order of the lamellar stacks.

To test biodegradability, PHB cast films were placed inside an all-purpose gardening soil (pH = 7.0) kept moist at 100% relative humidity for a period of about 2 months.

The soil was not added with other organic substances or microorganisms in order to keep the degradation media as similar as possible to the ground which is located in home gardens, it is already well known that microbial degradation[46] speeds up the rate of degradation, especially when there is a cationic clay as Cloisite in the polymer; in fact, the presence of microorganisms is a precondition for starting the subsequent hydrolysis and biodegradation.

The composites were weighed at 0, 20, and 40 days and only at the beginning and the end of the study period were analyzed by WAXD to assess the degree of crystallinity. It was not possible to record WAXD spectra at 20 days because the samples had undergone a considerable embrittelment and superficial alteration such as not to make them suitable for WAXD analysis and, therefore, it was necessary to grind the samples, an operation that was carried out only after 40 days when the crushing of the samples was such that it could no longer be sure, if repositioned in soil, to be able to collect all the fragments after a further period of time.

The obtained results are reported in Supporting Information, Table 2S.

All the samples show morphological alterations and a decrease in mass and crystallinity. The cast films, which show the most evident results are PHB2CL and PHB5CL, the samples containing Perkalite suffer a reduced degradative action; in fact, they show weight loss lower than that of neat PHB. All the films evidence a crystalline decrease, however, the samples containing Cloisite have a significant weight loss but a small decrement of crystallinity. On the contrary, samples with Perkalite do not show high degradability but have a large crystallinity decrement; this points out that the degradation process takes place primarily in the crystalline regions and then spreads over the amorphous ones, so there is a rapid decrease in the crystallinity degree when the weight loss is still moderate.

To understand the results obtained from the study of the biodegradation process, it is appropriate to discuss the effects of the type and amount of clay used to prepare the cast films.

It is well known that cationic clays, such as Cloisite,[47–49] may have both a barrier effect which improves the thermal stability and a catalytic effect that promotes the degradation of the polymer matrix, because these clays possess the catalytic sites of Al Lewis acids that facilitate hydrolytic fragmentation, this is not true for the anionic clays like Perkalite and this fact is consistent with the results obtained for the nanocomposites analyzed.

The hydrolytic fragmentation process is directly correlated to the weight loss; it is exactly this phenomenon that causes the

Table IV. Morphological Parameters of Lamellar Stacks, Obtained by SAXS Analysis of Cast Films

Sample	*N*	*C* (Å)	*A* (Å)	*D* (Å)	Φ_{SAXS} (%)	σ_C/C	σ_D/D
PHBcf	5	60	9	70	58	0.43	0.30
PHBcf5CL	7	58	11	69	57	0.34	0.30
PHBcf2PK	5	63	8	71	61	0.54	0.39
PHBcf5PK	5	57	13	70	55	0.47	0.33

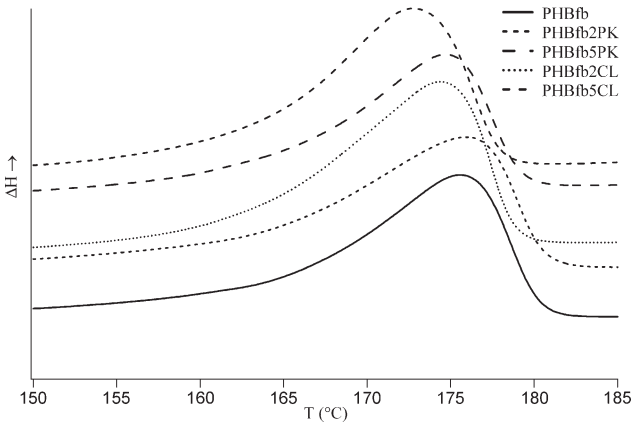

Figure 3. DSC curves of PHB electrospun fiber composites.

degradation and therefore the weight loss which makes the sample more fragile and likely to break.

The different amount of clay is instead responsible for a higher thermal stability if compared to the same nanocomposite containing 5% filler. It has been reported in the literature[50] that a low percentage of clay has an amplification of the barrier effect because its dispersion improves.

This also explains the decrease of biodegradability of PHBCL2 with respect to PHBCL5; on the contrary for the nanocomposites containing Perkalite, there is no noticeable effect on the biodegradability due to the different percentage of filler; this is probably due to the fact that the absence of catalytic sites of Al Lewis acids is the predominant reason of the low efficiency of Perkalite on the rate of biodegradation.

The study of electrospun fibers prepared from the same solution used to obtain the films, started determining the degree of crystallinity of PHB by DSC measurements because WAXD spectra were too poor. The thermograms are shown in Figure 3 and the results in Supporting Information, Table 3S.

In this case, the crystallization that occurs quickly during the electrospinning process prevents the clay to act as a nucleating agent, as in the case of cast films, and the effect of hindrance overrides to the regular organization of macromolecules. The results show a decrease of crystallinity for the fibers loaded with clay, more evident in those containing 5% nanofiller.

It was possible to determine the lamellar morphology of the fiber samples only for not loaded PHB; in fact, SAXS spectra of the samples containing clay are characterized by peaks of low intensity and large broadening as reported for PHBcf2CL. This does not allow accurate processing and indicates that the clay prevents the formation of ordered lamellar stacks.

The discussion of the results of the SAXS sample of neat PHB fiber must be made with respect to the cast films prepared from the same solution.

It is possible to point out that the percentage of crystallinity is a little bit higher (Table V) than that of the cast film samples (Table IV) with a lamellar morphology characterized by a higher long period and ordered stacks containing a large number of lamellae.

Table V. Morphological Parameters of the Lamellar Stacks Obtained by SAXS Analysis of PHB Fibers

Sample	*N*	*C* (Å)	*A* (Å)	*D* (Å)	Φ_{SAXS} (%)	σ_C/C	σ_D/D
PHBfb	22	66	32	98	67	0.48	0.36

The process of preparation of the samples from the solution is therefore critical for the lamellar morphology in the solid state; in fact, in the cast films, there is the formation of small stacks consisting of thin lamellae and small amorphous layer, while in the fiber samples, there are thicker amorphous layers within the lamellar stacks.

Through the analysis of the SAXS spectra, it was also possible to study the dispersion of the clay inside the fibers and compare its morphology to that of the pristine clay.

The results reported in Table VI allow to highlight that no phenomenon of intercalation can be observed in the fibers. Such a phenomenon probably occurs when the solution is prepared and it is maintained in the formation of cast films, in which the solidification process is slowly achieved. During the electrospinning process, the solidification takes place in a very short time so there is a reassemble of the stacks of clay into small tactoids with an average number of layers around 10.

From a macroscopic point of view, the material collected during electrospinning presents the characteristic compactness of a nonwoven fabric with the fibers randomly oriented in the sample without clay and in those containing Cloisite. Fibers filled with Perkalite are hollow and form coiled macrostruttures. The macroscopic morphology of the fibers can be observed in Figures 4–6 showing the images collected by optical (a,c) and scanning electron (b,d) microscope. Figure 7 shows the SEM image with higher magnification which highlights the hollow structure of the fibers of PHBfb5PK and the distribution of Perkalite (white dots).

The fibers without clay have an average size around 2 μm and tend to be bigger than the fibers containing Cloisite (0.7 and 2 μm) but smaller than those containing Perkalite (4 μm and 8 μm); the higher the percentage of clay, the bigger the diameter of the electrospun fibers.

It is therefore evident that the type and amount of clay have great influence on the macroscopic morphology of the produced fibers.

Table VI. Morphological Parameters of the Clay Stacks Obtained by SAXS Analysis of Clays and PHB Fiber Composites

Sample	*N*	*C* (Å)	*A* (Å)	*D* (Å)	σ_C/C	σ_D/D
cloisite	∞	10	14	25	0.40	0.19
PHBfb2CL	10	10	15	25	0.31	0.22
PHBfb5CL	10	10	15	25	0.31	0.22
perkalite	∞	14	20	34	0.36	0.26
PHBfb2PK	10	14	20	34	0.36	0.24
PHBfb5PK	10	14	20	34	0.36	0.24

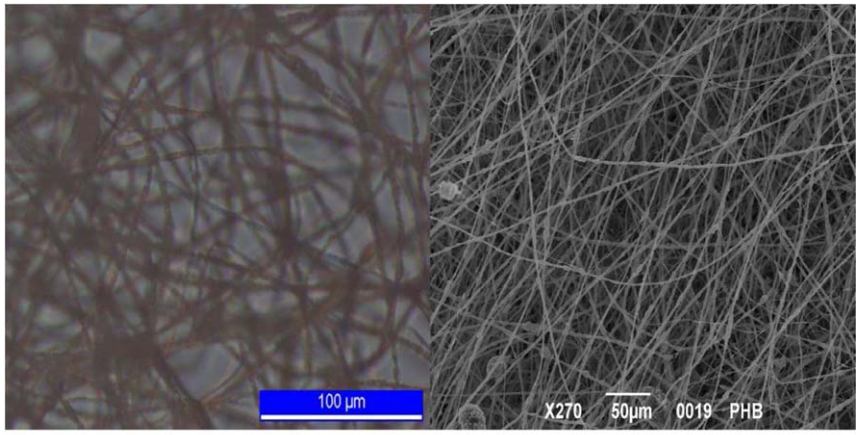

Figure 4. (a) POM and (b) SEM images of PHB electrospun fibers. [Color figure can be viewed in the online issue, which is available at wileyonlinelibrary.com.]

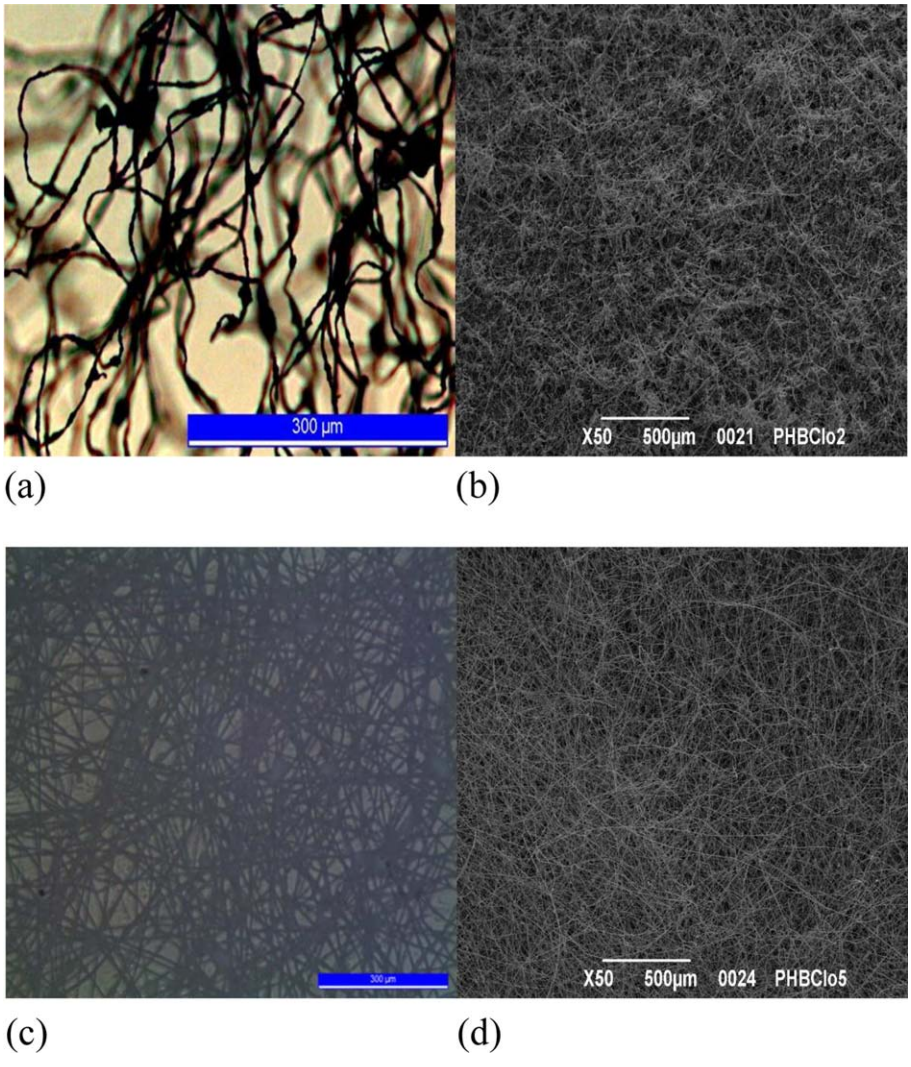

Figure 5. Images of PHB electrospun fibers filled with Cloisite: 2% ((a) POM, (b) SEM) and 5% ((c) POM, (d) SEM). [Color figure can be viewed in the online issue, which is available at wileyonlinelibrary.com.]

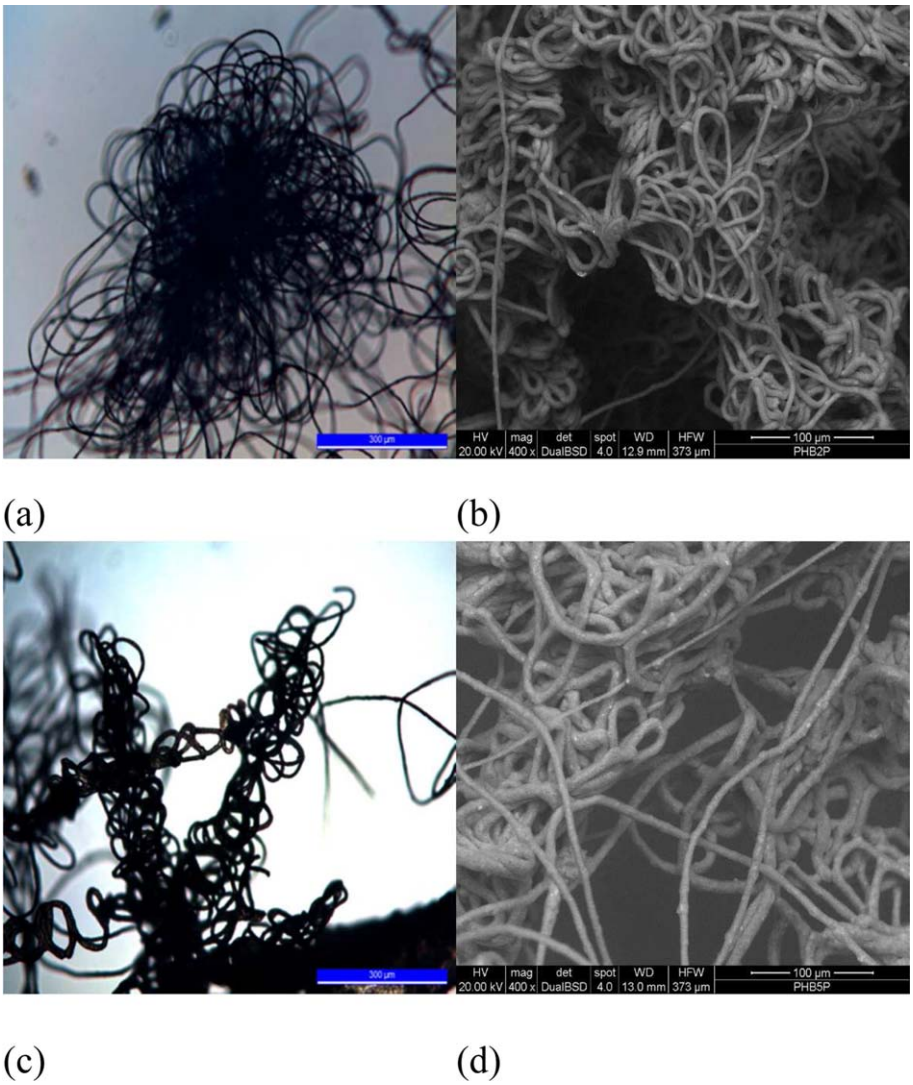

Figure 6. Images of PHB electrospun fibers filled with Perkalite: 2% ((a) POM, (b) SEM) and 5% ((c) POM, (d) SEM). [Color figure can be viewed in the online issue, which is available at wileyonlinelibrary.com.]

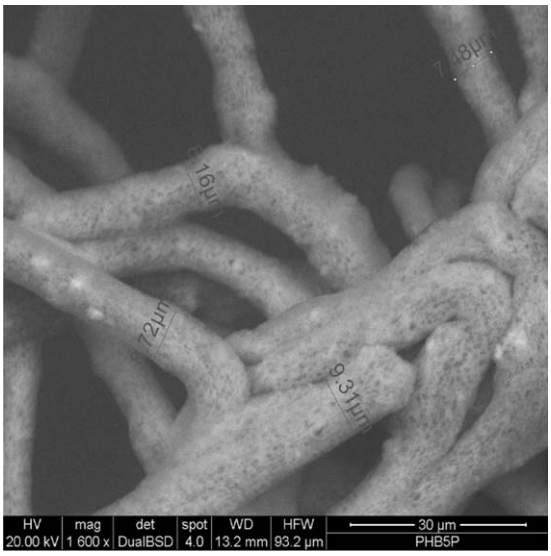

Figure 7. SEM image of PHB electrospun fibers filled with Perkalite 5%.

To investigate the role of the clay on the thermal behavior of PHB fibers, TGA measurements were performed which show that the decomposition temperature has a slight increase, compared to neat PHB (Supporting Information, Figure 2S and Table 4S) for the sample loaded with 2% Cloisite, while the same biodegradation temperature is measured for the sample with 5% and a decrease for those loaded with Perkalite.

Ultimately the addition of Cloisite tends to improve the thermal performance[14] of PHB, on the contrary Perkalite worsens it.

PCL/PHB Clay Composites

To assess how PHB fibers are arranged into the PCL matrix, after the preparation of the composite (Table II), the samples were broken in liquid nitrogen (in order to avoid the plastic deformation of the material) and then the SEM analysis was performed.

Figure 8 shows the SEM image of the fracture zone of the sample PCL/PHB_5CL which indicates a homogeneous distribution

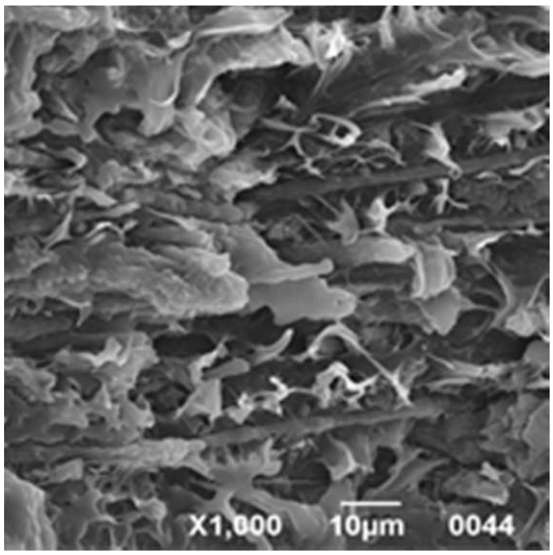

Figure 8. SEM image of the fractured PCL/PHB_5CL sample.

of the fibers included, without a preferred direction, within the matrix.

Thermal analysis of the composite samples by DSC allows to highlight (Table VII) a decrease, more evident in the samples containing Perkalite, of the melting temperature and a small increase in the degree of crystallinity compared to the unfilled PCL, it is possible to presume that there is a minimal effect of nucleation due to the fibers.

The analysis by SAXS of the sandwiched samples (Table VIII) shows that the morphological parameters remain substantially the same as the neat PCL. The structure of the lamellar stacks is therefore maintained, but there is a slight decrease in the long period, especially in samples containing Perkalite, this is associated with a decrease in the thickness of amorphous layers and it indicates an increase in the amorphous regions outside the lamellar stacks.

Confinement of clay in fibers has as a consequence that the morphology of the PCL remains substantially unchanged, unlike what happens in composites prepared by solvent casting.[29]

From SAXS data, it is also possible to note a small increase in the degree of crystallinity, as also indicated by DSC data. This is not detected by WAXD (Table IX) according to which there is a reduction of the crystallinity with the introduction of unfilled

Table VII. Melting Temperature (T_m) and Enthalpy (ΔH_m), Crystallinity Degree (X_{DSC}) of Sandwiched Samples

Sample	T_m (°C)	ΔH_m (J/g)	X_{DSC} (%)
PCL	62	75.7	53
PCL/PHB	59	75.1	53
PCL/PHB_2CL	58	76.3	54
PCL/PHB_5CL	58	77.9	55
PCL/PHB_2PK	56	77.9	55
PCL/PHB_5PK	56	79.7	56

Table VIII. Morphological Parameters of the Lamellar Stacks Obtained by SAXS Analysis of the Sandwiched Samples

Sample	*N*	*C* (Å)	*A* (Å)	*D* (Å)	Φ_{SAXS} (%)	σ_C/C	σ_D/D
PCL	30	86	60	146	59	0.39	0.28
PCL/PHB	30	88	56	144	61	0.42	0.31
PCL/PHB_2CL	32	90	53	143	63	0.40	0.29
PCL/PHB_5CL	30	89	56	144	61	0.42	0.30
PCL/PHB_2PK	30	88	53	141	63	0.41	0.30
PCL/PHB_5PK	27	87	53	140	61	0.42	0.31

fibers and values that come back to those of the neat PCL when the clays are also present. So it seems that the unfilled fibers induce a better organization in lamellar stacks, probably due to their more orderly macrostructure (Figure 4).

The clay inside the multicomponent composites is obviously confined within PHB fibers, its distribution and morphology are then described (Table VI) by data derived from SAXS analysis of the fibers. There is a different situation that if the clay had been dispersed by solvent casting directly into the PCL[29] matrix. In particular, it is to emphasize that the clay in fibers shows no phenomenon of intercalation, typical of nanocomposites prepared by solvent casting, and it is aggregated in tactoids containing about 10 stacks.

From TGA data, it is possible to determine (Table 5S) that the degradation temperature of the composites is observed in the same range of neat PCL.

The insertion of PHB fibers, however, results in an evident lowering (about 20°C) of this temperature and in a differentiated behavior according to type and amount of clay (Figure 9).

The presence of 2% Cloisite causes no change, while there is a significant decrease for the sample containing 5%. Even for the samples containing Perkalite, there is a decrease of T_{deg}, very marked (about 68°C) for the one containing 2%.

In particular, the addition to the PCL matrix of PHB fibers allows to decrease T_{deg}, but just a small amount of cloisite (2%) enables to bring T_{deg} back to that of the neat PCL; on the contrary, the same amount of Perkalite leads to a T_{deg} much lower.

Table IX. Weight Loss of Sandwiched Samples after 60 days of Biodegradation and Crystallinity Degree by Volume at Days 0 and 60

Sample	Weight loss (%) at day 60	Φ_{WAXD} (%) at day 0	Φ_{WAXD} (%) at day 60
PCL	39	52	57
PCL/PHB	0	47	47
PCL/PHB_2CL	0.3	50	50
PCL/PHB_5CL	9	52	52
PCL/PHB_2PK	0.4	50	52
PCL/PHB_5PK	0.6	53	51

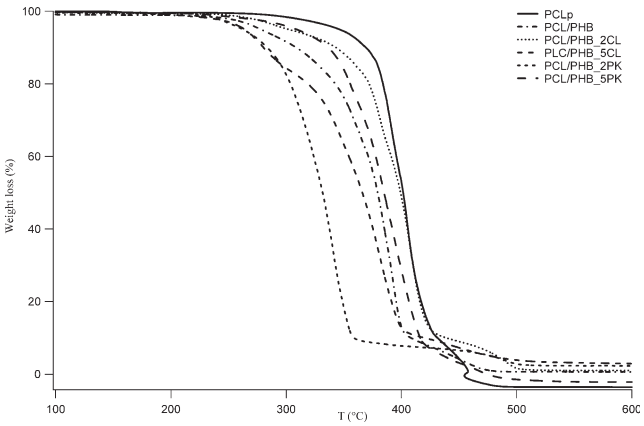

Figure 9. TGA curves of PCL/PHB/clay composites.

It is interesting to underline that the preparation of these multicomponent composites containing a very low amount of clays allows to modulate the properties of thermal stability of PCL as already detected[16,28,51] in the case of addition of larger amount of Cloisite not confined in fibers.

The data related to the degradation behavior of the composites in soil (Table IX) show that there is a very sensible weight decrease for neat PCL, which also presents an increase in crystallinity after 60 days, indicating that the amorphous regions are the most subjected to the process of degradation.

A dramatic slowdown in this process is observable with the introduction of PHB fibers, but for that containing 5% Cloisite. It is noteworthy that the crystallinity remains unchanged, so the degradation proceeds in the same way for all the material both in the amorphous and in the crystalline phase, even when there is the greatest weight loss, that is, in the sample PCL/PHB_5CL.

Once again a different behavior is detected from that of the composites prepared from solvent casting,[29] in which there is a delay of the start of biodegradation and a preferential attack of the amorphous regions, with a consequent increase in the degree of crystallinity. In the case of the multicomponent composites, the confinement of clay into the fibers leads again to a delay in the biodegradation process, but both the crystalline and amorphous regions are attacked and the degree of crystallinity remains unchanged.

The clay confined in the fibers cannot act as a fast promoter of the biodegradation process, probably because the first action is directed to the degradation of PHB fibers, which are internal to the PCL matrix, and thus protected from the external environment, in this case, the soil.

It is obvious that there is a delay with respect to the start of the biodegradation process in PHB films (Supporting Information, Table 2S) and PCL[29] containing clays not confined in fibers or neat PCL (Table IX).

The type and amount of clay and fibers in the matrix of PCL, therefore, allow to control the start of biodegradation. This can be useful for example in biodegradable packaging materials, in pharmaceutical controlled release systems, and other medical applications for which it is important that the biodegradable material can remain unchanged for a certain period of time.

The tensile properties of the composite materials were then analyzed (Table X). Also in this case, the behavior of PCL/PHB_5CL differs from the other ones; there is a considerable decrease in the elastic modulus with a relative increase of strain at break. In general, for the other composites, there is still an increase of ductility even if the elastic modulus is substantially unchanged, a behavior already reported for PCL nanocomposites.[29]

CONCLUSIONS

The preparation of multicomponent composites based on PCL gives as a result a change of the properties of the neat polymer, even if the clay is introduced in very low amount and confined within the fibers of PHB, in fact the presence of both clay and fibers induces changes in the behavior of the PCL matrix.

From the analysis of the data relating to the degree of crystallinity obtained by DSC, WAXD, and SAXS, we can assume that the unfilled fibers induce a better organization in lamellar stacks, probably due to their more orderly macrostructure, even if the overall degree of crystallinity tends to decrease.

The confinement of clay in fibers has as a consequence that the morphology of the PCL remains substantially unchanged and there is no phenomenon of intercalation, unlike what happens in composites prepared by solvent casting,

It is again the presence of clay stuck inside PHB fibers that leads to a delay in the biodegradation process, but both the crystalline and amorphous regions are attacked and the degree of crystallinity remains unchanged.

The filled PHB fibers allow to modulate the properties of thermal stability of PCL and prevent the biodegradation process for

Table X. Tensile Properties of the Sandwiched Composites

Sample	Modulus (MPa)	Stress at yield (MPa)	Strain at yield (%)	Stress at break (MPa)	Strain at break (%)
PCL	440 ± 3	6.0 ± 0.3	95 ± 4	5.6 ± 0.2	96 ± 4
PCL/PHB	436 ± 3	9.0 ± 0.3	106 ± 4	1.4 ± 0.1	112 ± 4
PCL/PHB_2CL	461 ± 3	10.3 ± 0.4	116 ± 5	10.3 ± 0.4	116 ± 5
PCL/PHB_5CL	183 ± 7	3.1 ± 0.1	97 ± 5	1.2 ± 0.1	127 ± 6
PCL/PHB_2PK	444 ± 3	7.1 ± 0.2	104 ± 3	7.1 ± 0.2	104 ± 3
PCL/PHB_5PK	397 ± 4	6.3 ± 0.3	110 ± 4	6.0 ± 0.3	111 ± 4

all composites except for the one containing PHB fibers with 5% Cloisite.

The same sample PCL/PHB_5CL shows the peculiar mechanical behavior of a considerable decrease in the elastic modulus with a relative increase of strain at break, which is not found in the other samples.

Although the purpose of this article concerns the study of PCL composites, it was also possible to draw interesting conclusions from the study of films and fibers prepared from the same solution of PHB, related to the difference in their morphology.

It is obvious that the dissolution of the polymer in the solvent produces the effect of disruption of the lamellar morphology and crystalline order; it also allows the penetration of the polymer within the layers of clay allowing the occurrence of the phenomenon of intercalation.

The different way to obtain the material in the solid state, however, has as a consequence a different lamellar morphology and a different organization of the clay.

The process used to obtain films occurs through slow evaporation of the solvent; on the contrary, the formation of fibers through electrospinning is characterized by fast solidification and stretching.

Besides, the phenomenon of intercalation is maintained only in the cast film composites, while in the fibers there is a reassemble of the stacks of clay into tactoids, probably due to the fast spinning process.

REFERENCES

1. Anderson, A. J.; Dawes, E. A. *Microbiol. Rev.* **1990**, *54*, 450.
2. Pan, P.; Inoue, Y. *Prog. Polym. Sci.* **2009**, *34*, 605.
3. Dawes, E. A. *Biosci. Rep.* **1998**, *8*, 537.
4. Yang, K. K.; Wang, X. L.; Wang, Y. Z. *J. Ind. Eng. Chem.* **2007**, *13*, 485.
5. Satoh, Y.; Tajima, K.; Tannai, H.; Munekata, M. *J. Biosci. Bioeng.* **2003**, *95*, 335.
6. Orts, W. J.; Marchessault, R. H.; Bluhm, T. L.; Hamer, G. K. *Macromolecules* **1990**, *23*, 5368.
7. Cornibert, J.; Marchessault, R. H. *J. Mol. Biol.* **1972**, *71*, 735.
8. Suttiwijitpukdee, N.; Sato, H.; Zhang, J.; Hashimoto, T.; Ozaki, Y. *Polymer* **2011**, *52*, 461.
9. Yamane, H.; Terao, K.; Hiki, S.; Kawahara, Y.; Kimura, Y.; Saito, T. *Polymer* **2001**, *42*, 7873.
10. Hong, S. G.; Gau, T. H.; Huang, S. C. *J. Therm. Anal. Calorim.* **2011**, *103*, 967.
11. Chen, B. Q.; Evans, J. R. G. *Macromolecules* **2006**, *39*,747.
12. Long, Y. Biodegradable Polymer Blends and Composites from Renewable Resources; Wiley, **2007**.
13. Galego, N.; Rozsaa, C.; Sanchez, R.; Fung, J.; Vazquez, A.; Tomas, J. S. *Polym. Test.* **2000**, *19*, 485.
14. Maiti, P.; Batt, C. A.; Giannelis, E. P. *Biomacromolecules* **2007**, *8*, 3393.
15. Michel, A. T.; Billington, S. L. *Polym. Degrad. Stab.* **2012**, *97*, 870.
16. Lepoittevin, B.; Devalckenaere, M.; Pantoustier, N.; Alexandre, M.; Kubies, D.; Calberg, C.; Jerome, R.; Dubois, P. *Polymer* **2002**, *43*, 4017.
17. Pantoustier, N.; Lepoittevin, B.; Alexandre, M.; Kubies, D.; Calberg, C.; Jerome, R.; Dubois, P. *Polym. Eng. Sci.* **2002**, *42*, 1928.
18. Di Maio, E.; Iannace, S.; Sorrentino, L.; Nicolais, L. *Polymer* **2004**, *45*, 8893.
19. Gorrasi, G.; Tortora, M.; Vittoria, V.; Pollet, E.; Alexandre, M.; Dubois, P. *J. Polym. Sci. Part B: Polym. Phys.* **2004**, *42*, 1466.
20. Pucciariello, R.; Villani, V.; Belviso, S.; Gorrasi, G.; Tortora, M.; Vittoria, V. *J. Polym. Sci. Part B: Polym. Phys.* **2004**, *42*, 1321.
21. Lee, S. K.; Seong, D. G.; Youn, J. R. *Fibres polym.* **2005**, *6*, 289.
22. Gain, O.; Espuche, E.; Pollet, E.; Alexandre, M.; Dubois, P. *J. Polym. Sci. Part B: Polym. Phys.* **2005**, *43*, 205.
23. Homminga, D.; Goderis, B.; Dolbnya, I.; Groeninckx, G. *Polymer* **2006**, *47*, 1620.
24. Chrissafis, K.; Antoniadis, G.; Paraskevopoulos, K. M.; Vassiliou, A.; Bikiaris, D. N. *Compos. Sci. Technol.* **2007**, *67*, 2165.
25. Kiersnowski, A.; Gutmann, J. S.; Pigtowski, J. *J. Polym. Sci. Part B Polym. Phys.* **2007**, *45*, 2350.
26. Shibata, M.; Teramoto, N.; Someya, Y.; Tsukao, R. *J. Appl. Polym. Sci.* **2007**, *104*, 3112.
27. Wu, K.; Wu, C.; Chang, J. *Process. Biochem.* **2007**, *42*, 669.
28. Marras, S. I.; Kladi, K. P.; Tsivintzelis, L.; Zuburtikudis, I.; Panayiotou, C. *Acta Biomaterialia* **2008**, *4*, 756.
29. Neppalli, R.; Causin, V.; Marega, C.; Saini, R.; Mba, M.; Marigo, A. *Polym. Eng. Sci.* **2011**, *51*, 1489.
30. Neppalli, R.; Marega, C.; Marigo, A.; Bajgai, M. P.; Kim, H. Y.; Causin, V. *Eur. Polym. J.* **2010**, *46*, 968.
31. Neppalli, R.; Marega, C.; Marigo, A.; Bajgai, M. P.; Kim, H. Y.; Causin, V. *Polymer* **2011**, *52*, 4054.
32. Akita, S.; Einaga, Y.; Miyiaki, Y.; Fujita, H. *Macromolecules* **1976**, *9*, 774.
33. Marega, C.; Causin, V.; Marigo, A.; Ferrara, G.; Tonnaer, H. *J. Nanosci. Nanotechnol.* **2009**, *9*, 2704.
34. Neppalli, R.; Marega, C.; Marigo, A.; Bajgai, M. P.; Kim, H. Y.; Ray, S. S.; Causin, V. *J. Mater. Res.* **2012**, *27*, 1399.
35. Hindele, A. M.; Johnson, D. J. *J. Phys. D: Appl. Phys.* **1971**, *4*, 259.
36. Vonk, C. G.; Pijpers, A. P. *J. Polym. Sci. Part B: Polym. Phys.* **1985**, *23*, 2517.
37. Vonk, C. G. *J. Appl. Crystallogr.* **1973**, *6*, 81.
38. Vonk, C. G. *J. Appl. Crystallogr.* **1971**, *4*, 340.
39. Marega, C.; Marigo, A.; Cingano, G.; Zannetti, R.; Paganetto, G. *Polymer* **1996**, *37*, 5549.
40. Hosemann, R.; Bagchi, S. N. *Direct Analysis of Diffraction by Matter*; North Holland: Amsterdam, **1962**.
41. Yu, L.; Cebe, P. *Polymer* **2009**, *50*, 2133.

42. Marega, C.; Marigo, A.; Causin, V. *J. Appl. Polym. Sci.* **2003**, *90*, 2400.

43. Causin, V.; Marega, C.; Marigo, A.; Ferrara, G. *Polymer* **2005**, *46*, 9533.

44. Marega, C.; Causin, V.; Marigo, A. *J. Appl. Polym. Sci.* **2008**, *109*, 32.

45. Causin, V.; Marega, C.; Marigo, A.; Ferrara, G.; Idyatullina, G.; Fantinel, F. *Polymer* **2006**, *47*, 4773.

46. Singh, N. K.; Purkayastha, B. D.; Roy, J. K.; Banik, R. M.; Yashpal, M.; Singh, G.; Malik, S.; Maiti, P. *Appl. Mater. Interfaces* **2010**, *2*, 69.

47. Zhao, C.; Qin, H.; Gong, F.; Feng, M.; Zhang, S.; Yang, M. *Polym. Degrad. Stab.* **2005**, *87*, 183.

48. D'amico, D. A.; Manfredi, L. B.; Cyras, P. C. *J. Appl. Polym. Sci.* **2012**, *123*, 200.

49. Bordes, P.; Pollet, E.; Avérous, L. *Prog. Polym. Sci.* **2009**, *34*, 125.

50. Zhang, R.; Huang, H.; Yang, W.; Xiao, X.; Yuan, H. *Compos.: Part A* **2012**, *43*, 547.

51. Lim, S. T.; Hyun, Y. H.; Lee, C. H.; Choi, H. J. *J. Mater. Sci. Lett.* **2003**, *22*, 299.